Geophysical Research Letters

Supporting Information for

Anthropogenic influence on recent severe autumn fire weather in the west coast of the United States

Linnia R. Hawkins[1], John T. Abatzoglou[2], Sihan Li[3,4], David E. Rupp[5]

[1]Forest Ecosystems & Society Department, Oregon State University, Corvallis, OR, USA, [2]Management of Complex Systems Department, University of California Merced, Merced, CA, USA, [3]Environmental Change Institute, School of Geography and the Environment, University of Oxford, Oxford, UK, [4]Oxford e-Research Centre, University of Oxford, Oxford, UK, [5]Oregon Climate Change Research Institute, College of Earth, Ocean, and Atmospheric Science, Oregon State University, Corvallis, OR, USA

Contents of this file

Introduction

This supporting information contains additional technical details of the methodologies used in sections S1-S3 as well as figures S1-S8 and tables S1-S5.

Section S1. Experimental design

The analyses of this study are based on two sets of attribution experiments, one using modelled outputs to calculate fire weather indices (*fire weather experiment*) and the other using modelled outputs to perform the wind analysis (*wind experiment*). Each set of experiments consisted of an ensemble of simulations representing modern-era climate conditions, referred to as actualClim, and an ensemble of simulations representing pre-industrial climate (i.e. without anthropogenic influence), referred to as naturalClim. The actualClim and naturalClim ensembles covered the same time period, with the actualClim ensembles using observed concentrations of greenhouse gases and observation-based SSTs and sea ice fractions (SIC) from the Operational Sea Surface Temperature and Sea Ice Analysis (OSTIA; Donlon et al. 2012). Whereas the naturalClim ensembles used pre-industrial level greenhouse gases and pre-industrial SST and SIC, constructed by removing anthropogenic signals from the OSTIA observed values. Thirteen estimates of anthropogenic SST (deltaSST) warming patterns were used, 12 from CMIP5 models,

and 1 from the multi-model mean constructed from these 12 models. The deltaSST calculations are detailed in Schaller et al. (2014).

The *fire weather experiment* covered Sep2016-Dec2018, with Sep through Nov 2016 excluded from the analysis due to the lack of antecedent information needed for calculating fuel moisture in autumn 2016. The *wind experiment* covered Sep2017-Dec2018. Model outputs consisted of daily values (precipitation) or instantaneous values (10-m wind speed, 2-m temperature, 2-m relative humidity from the *fire weather experiment* and wind velocity, temperature, geopotential height at various pressure levels from the *wind experiment*) at 21Z (1300 LST) corresponding to the approximate times used in calculating daily fire danger rating systems.

S2. Comparison of 700-hPa wind climatology from HadAM-RM3p and reanalysis

We compared wind climatology between the HadAM-RM3p ensemble and ECMWF ReAnalysis 5 (ERA5; Hersbach et al., 2020) because ERA5 has a similar horizontal resolution (30 km) to HadRM3p (~25 km) and is the state-of-the-art reanalysis. We used the years 1979-2019 from ERA5. From the HadAM-RM3p ensemble, the distribution of winds represents internal atmospheric variability in the year 2018 only, so it is expected that the distribution is narrower than it would be if the SSTs from 1979 to 2019 were used as the boundary conditions to HadAM-RM3p.

From the *wind experiment* with HadAM-RM3p, winds on several pressure levels were saved daily at 21 Z for 402 initial condition ensemble members; the sample size = 12,060 wind fields per pressure level per month (402 ensemble members × 30 days per month).

Figures S1-S3 show frequency distributions of wind speed and direction, as wind roses, for the months of autumn (September, October, and November) at 700-hPa for example locations in Regions ORa, CAa, and CAd, respectively. The precise locations are shown in Fig. 4d and identified by the solid black circle in each region.

S3. Identification and examination of offshore downslope winds in the HadAM-RM3p ensemble

In the HadAM-RM3p ensemble, we identified conditions suitable for offshore, downslope winds (ODWs) in six regions from northern Oregon to southern California, with each region consisting of 16 model grid cells in a 4x4 matrix (See region locations in Fig. 4d). We adapted the method of Abatzoglou et al. (2021b) to identify instances of such conditions based on the cross-barrier 700-hPa horizontal wind speed $u \geq 13$ m s-1 and the 700-hPa vertical wind speed $\omega \geq 0.6$ Pa s-1 at 21 Z in a grid cell. Within a region, the u and ω criteria did not have to be met in the same grid cell for the instance to qualify. The cross-barrier wind direction varied by region to accommodate the primary direction of offshore flow and orientation of orography: 90°, 60°, and 45° for the Cascades, Sierras, and Transverse Ranges, respectively. We added the criterion of near-surface $RH \leq 30\%$ (e.g., Edinger et al., 1964; Smith et al., 2018) to further constrain focus on wind events that yield elevated fire weather potential.

We further determined if the climate model would simulate lower troposphere and near-surface conditions associated with ODWs as, or more, extreme as those during several of the recent large autumn wildfires in California and Oregon. We used the same general method for identifying ODWs described above but considered extreme ODW using more stringent criteria: Cross-barrier 700-hPa wind speed > 18 m s^{-1}, 700-hPa $\omega > 1.5$ Pa s^{-1}, and near-surface $RH < 20\%$.

Simulated ODW frequency in autumn varied regionally from < 1 day per autumn in the Oregon Cascades (ORa and ORb) to nearly 3 days per autumn in Transverse Ranges (CAd) (Table S1). Along the Sierra Nevada, frequencies decreased from north to south, consistent with diagnostics from ERA5 (Abatzolgou et al., 2021b). However, frequencies were sensitive to the selected

cross-barrier wind direction and the exact locations of the analysis regions, so precise comparisons between regions should not be made based on these results.

The HadAM-RM3p actualClim ensemble contained instances of extreme ODWs in all regions in autumn (Table S1). Extreme ODWs were rarest in the Oregon Cascades (0.09 instances per autumn on average), and most frequent in Transverse Ranges (0.96 instances per autumn).

Figures S4-S6 show latitudinal profiles of wind velocity and air temperature in the lower troposphere during examples of extreme ODWs in Regions ORa, CAa, and CAd, respectively. The figures show one snapshot of extreme ODWs for each region from three unique model simulations to illustrate the signature of ODWs. In the Oregon Cascades example (ORa; Fig. S4), the ODW criteria were met on three consecutive days at 21 Z and the maximum 700-hPa cross-barrier wind speed and ω were 21.0 m s^{-1} and 2.2 Pa s^{-1}, respectively while the minimum surface *RH* was 6.1%. In the Sierras example (CAa; Fig. S5), the criteria were met on two consecutive days at 21 Z and the maximum 700-hPa cross-barrier wind speed and ω were 34.6 m s^{-1} and 5.3 Pa s^{-1}, respectively, while the minimum surface *RH* was 9.9%. Fig. S5 also shows the characteristic temperature inversion that can develop during these events (e.g., Abatzoglou et al. 2021b) persisting into the afternoon. For the Transverse Ranges example (CAd; Fig. S6), the criteria were met on two consecutive days at 21 Z and the maximum 700-hPa cross-barrier wind speed and ω were 29.8 m s^{-1} and 5.1 Pa s^{-1}, respectively while the minimum surface *RH* was 9.2%.

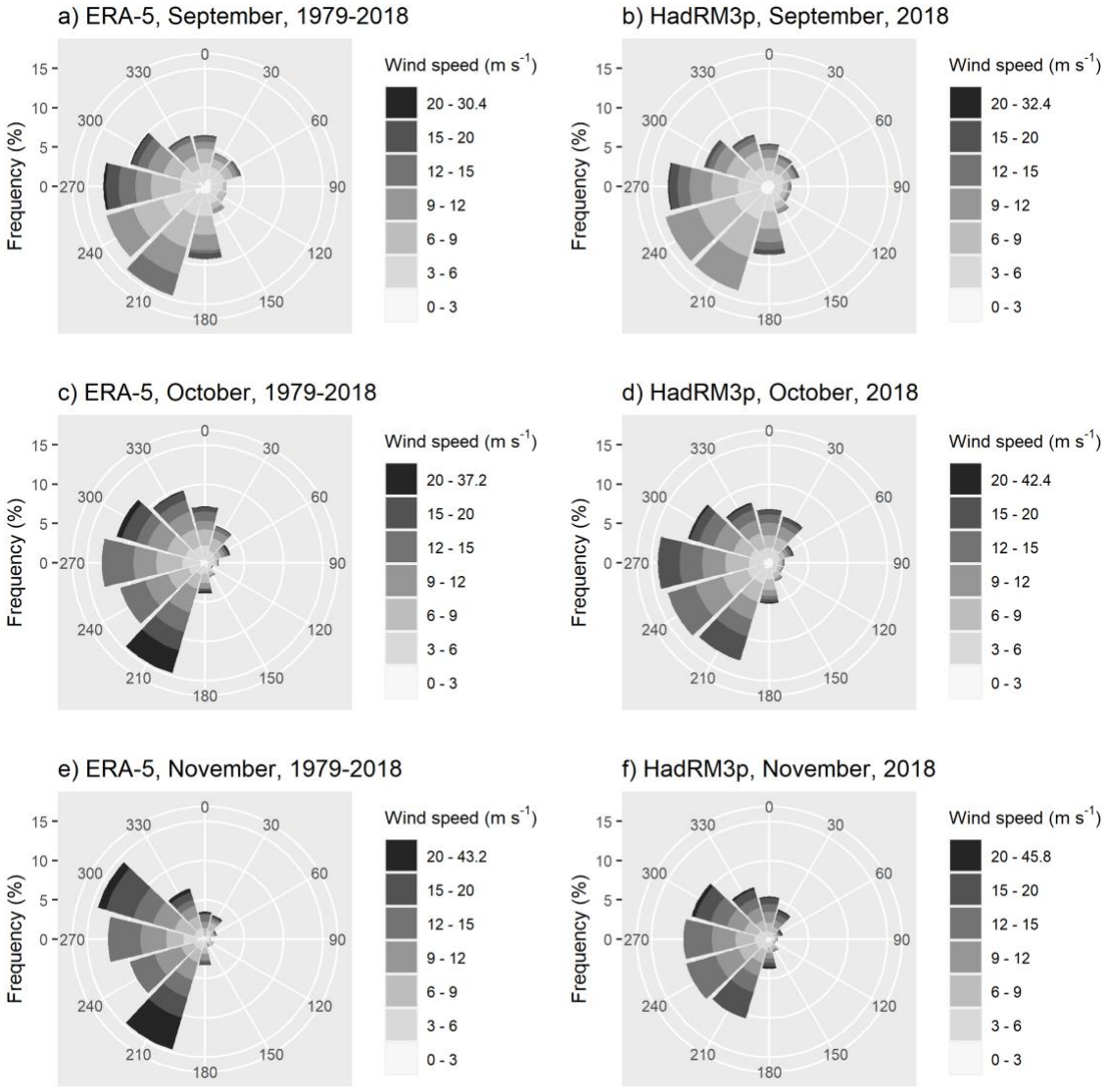

Figure S1. Frequency distribution of 700-hPa wind speed and wind direction at 21 Z for a location in Region ORa in **(a, b)** September, **(c, d)** October, and **(e, f)** November from **(a, c, e)** ERA5, 1979-2019 (-122.25°E, 44.75°N) and **(b, d, f)** and the HadAM-RM3p 402-member ensemble (-122.3733°E, 44.8175°N).

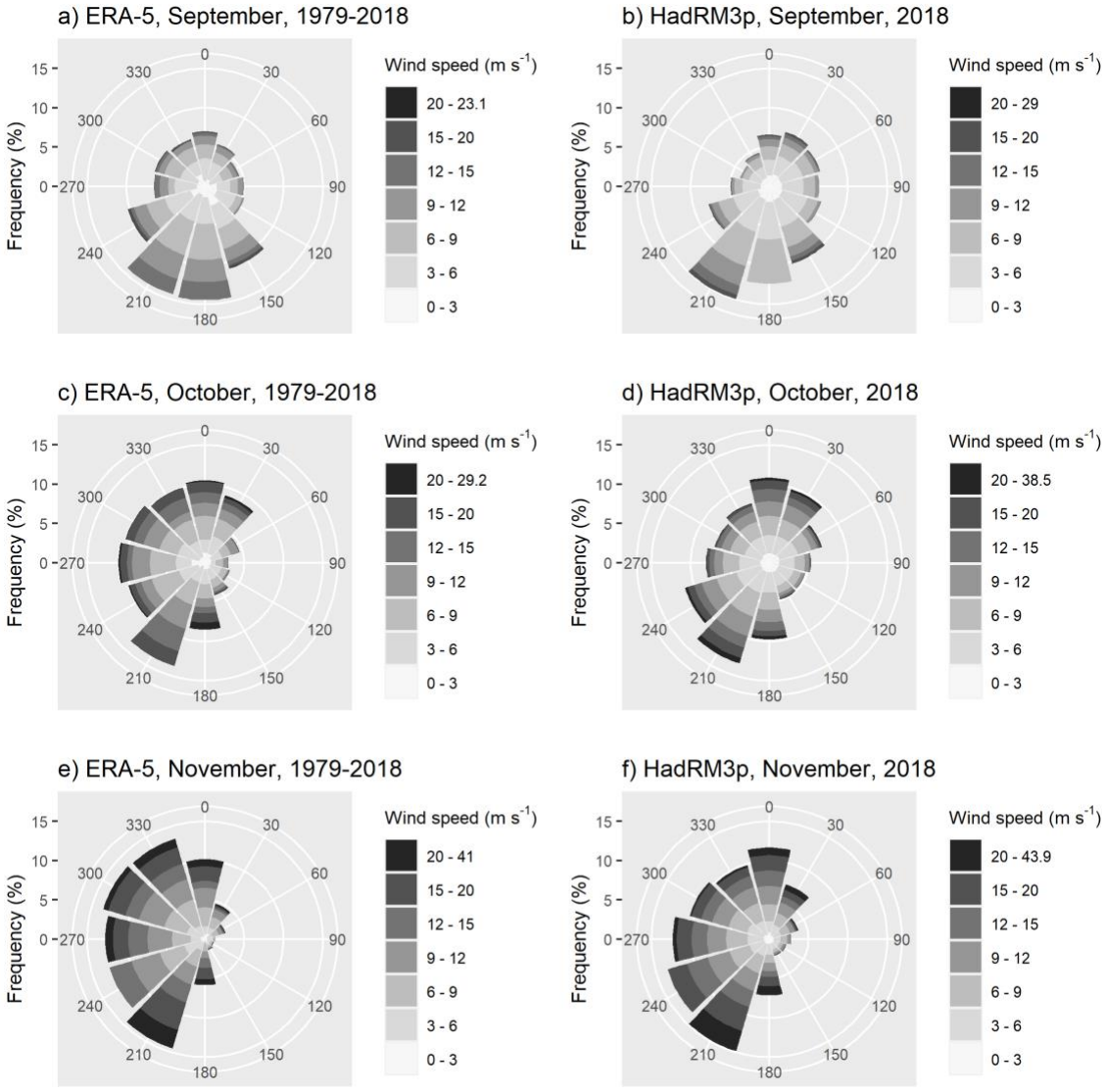

Figure S2. Fame as Figure S2 but for a location in Region CAa from ERA5 (-121.75°E, 40.00°N) and HadAM-RM3p (-121.7413°E, 39.9799°N).

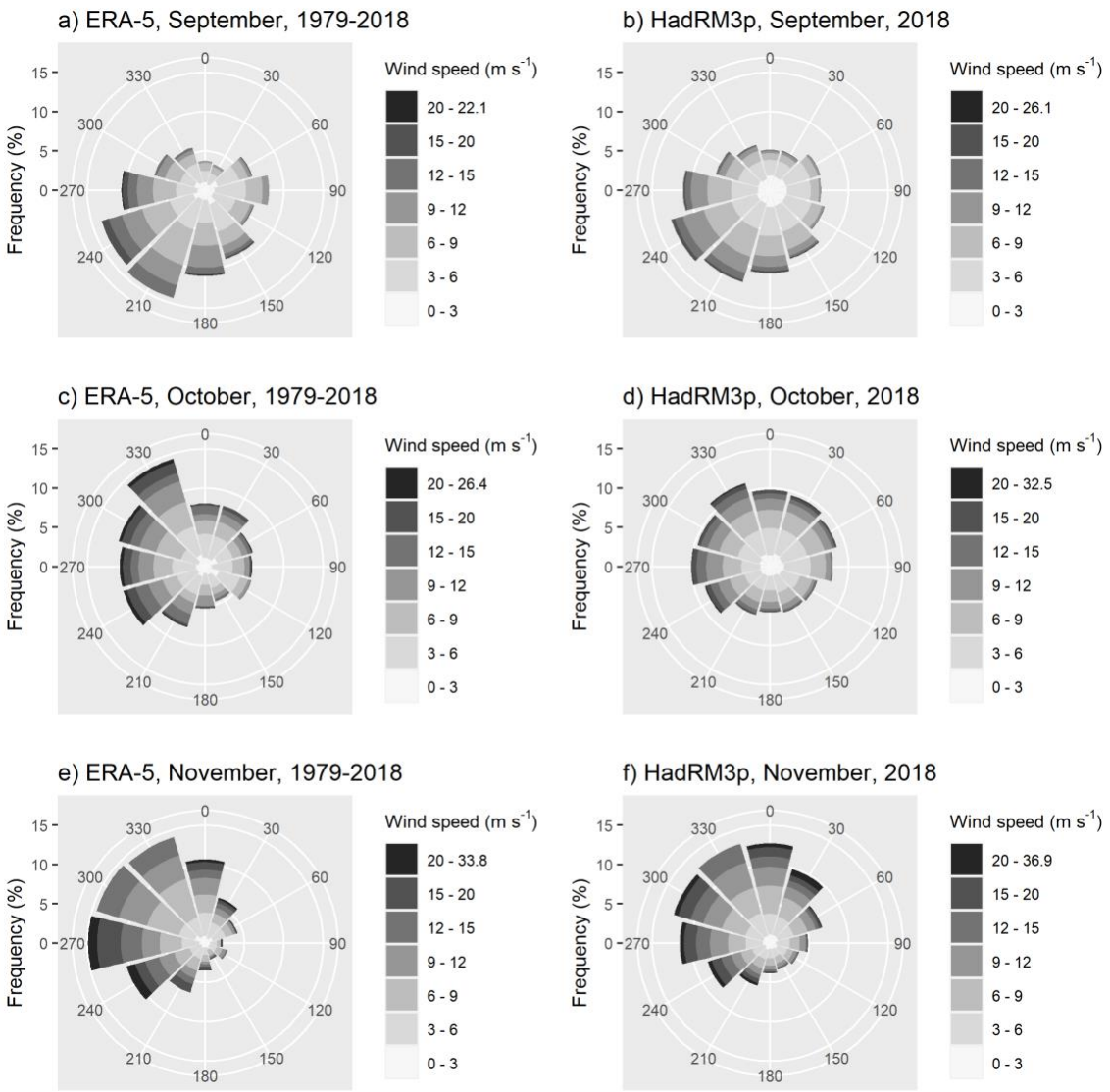

Figure S3. Same as Figure S2 but for a location in Region CAd from ERA5 (-118.50°E, 34.50°N) and HadAM-RM3p (-118.5516°E, 34.4359°N).

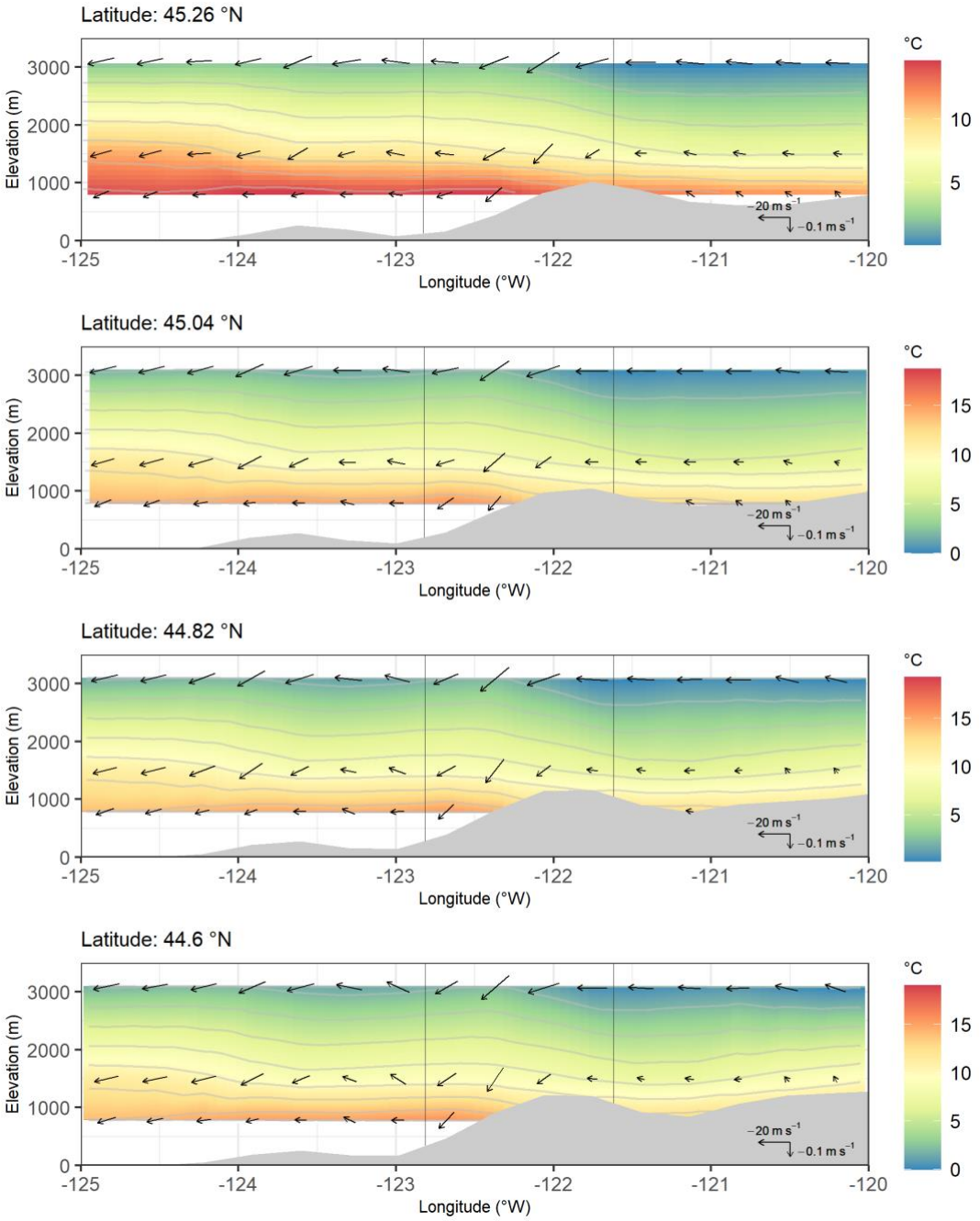

Figure S4. Example of simulated temperature and winds along 4 latitudinal transects at 21 Z meeting criteria for extreme downslope wind conditions on an autumn day in Region ORa (see Figure 4d). Gray shading shows land. The two vertical gray lines mark the east and west boundaries of the 4 x 4 grid used when determining extreme downslope wind conditions. Temperature was bilinearly interpolated from points at the 925, 850 and 700-hPa pressure levels. Latitude designations are approximate for each panel because the regional model grid is not oriented along lines of global latitude and longitude.

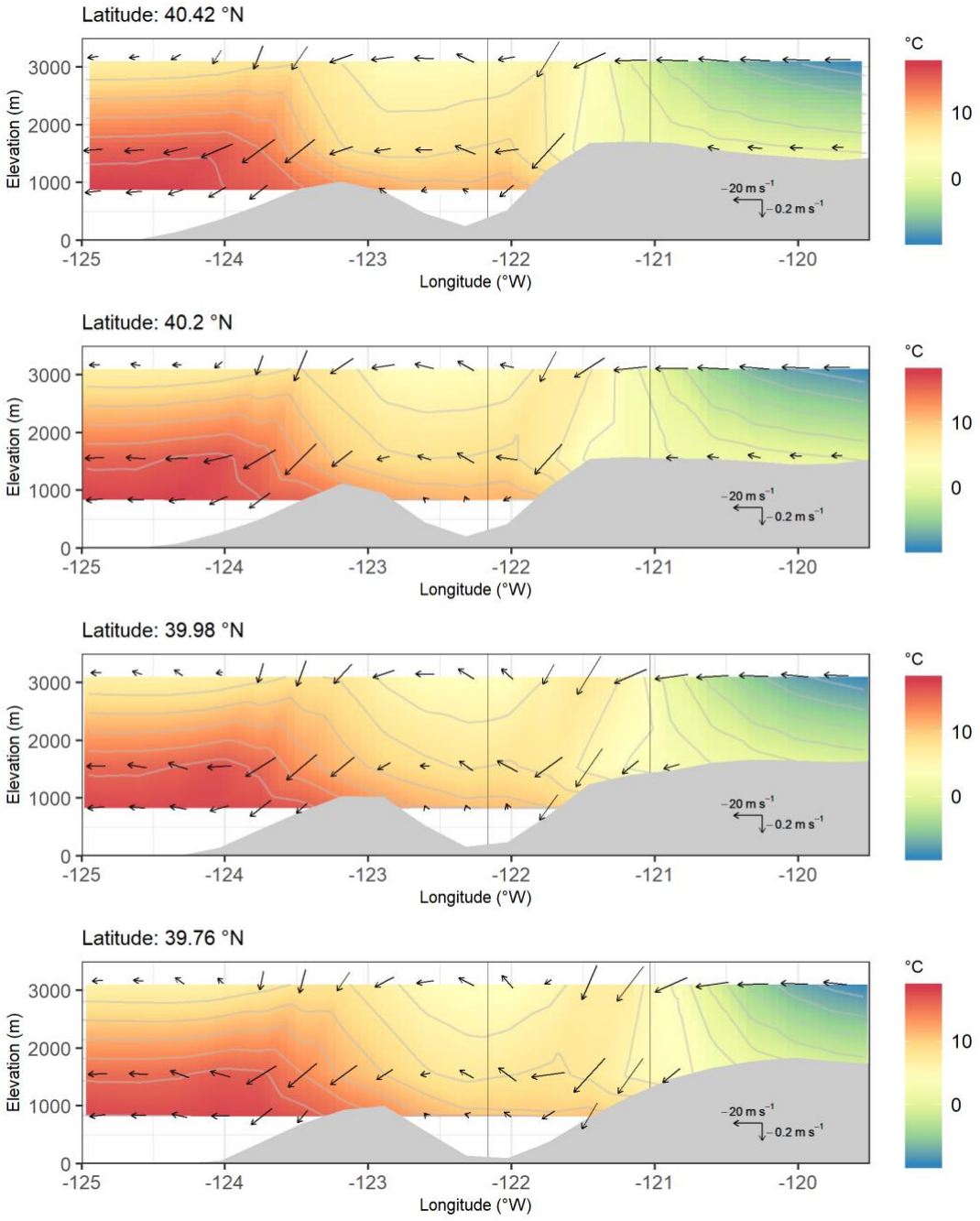

Figure S5. Same as Fig. S4 but for Region CAa.

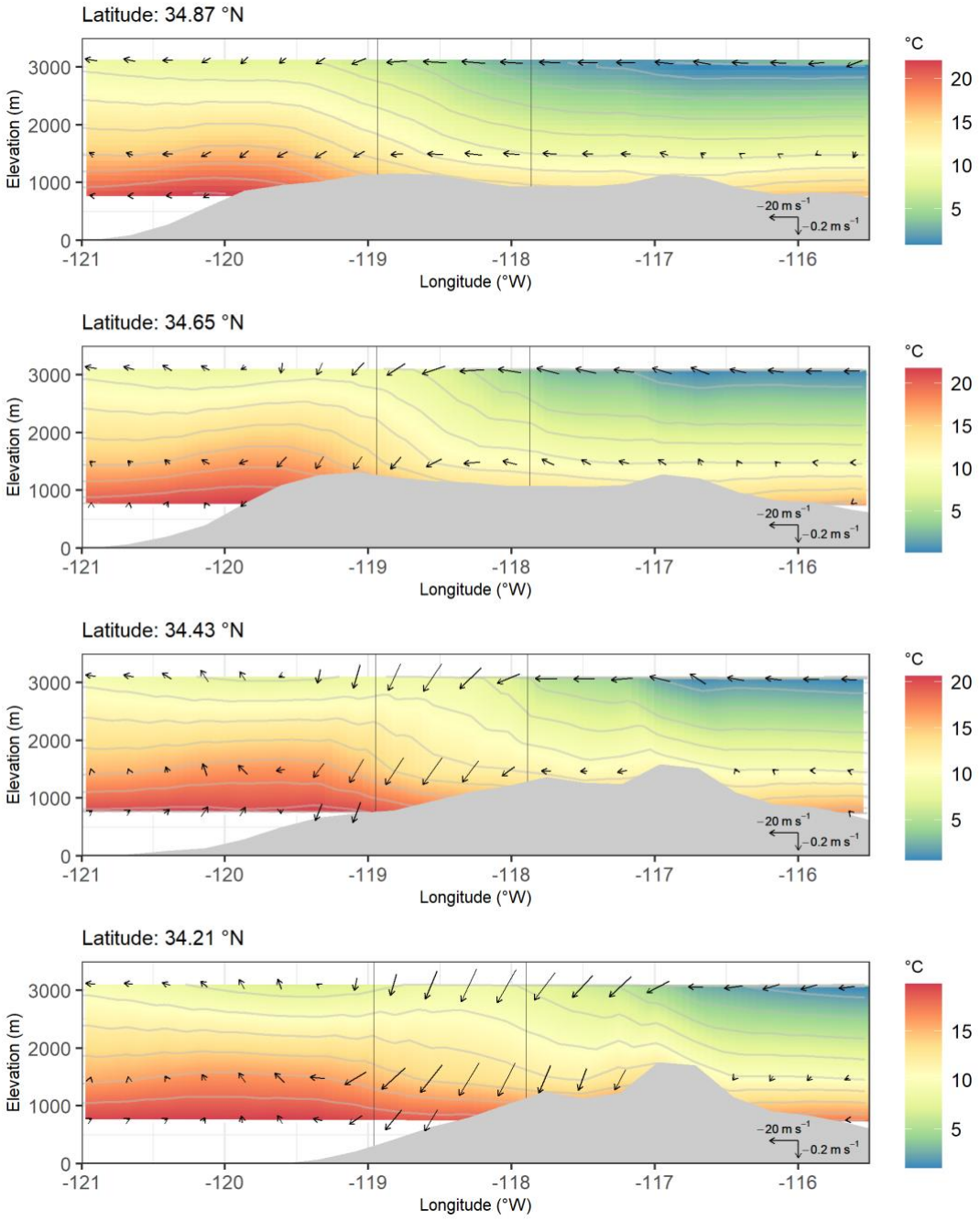

Figure S6. Same as Fig. S4 but for Region CAd.

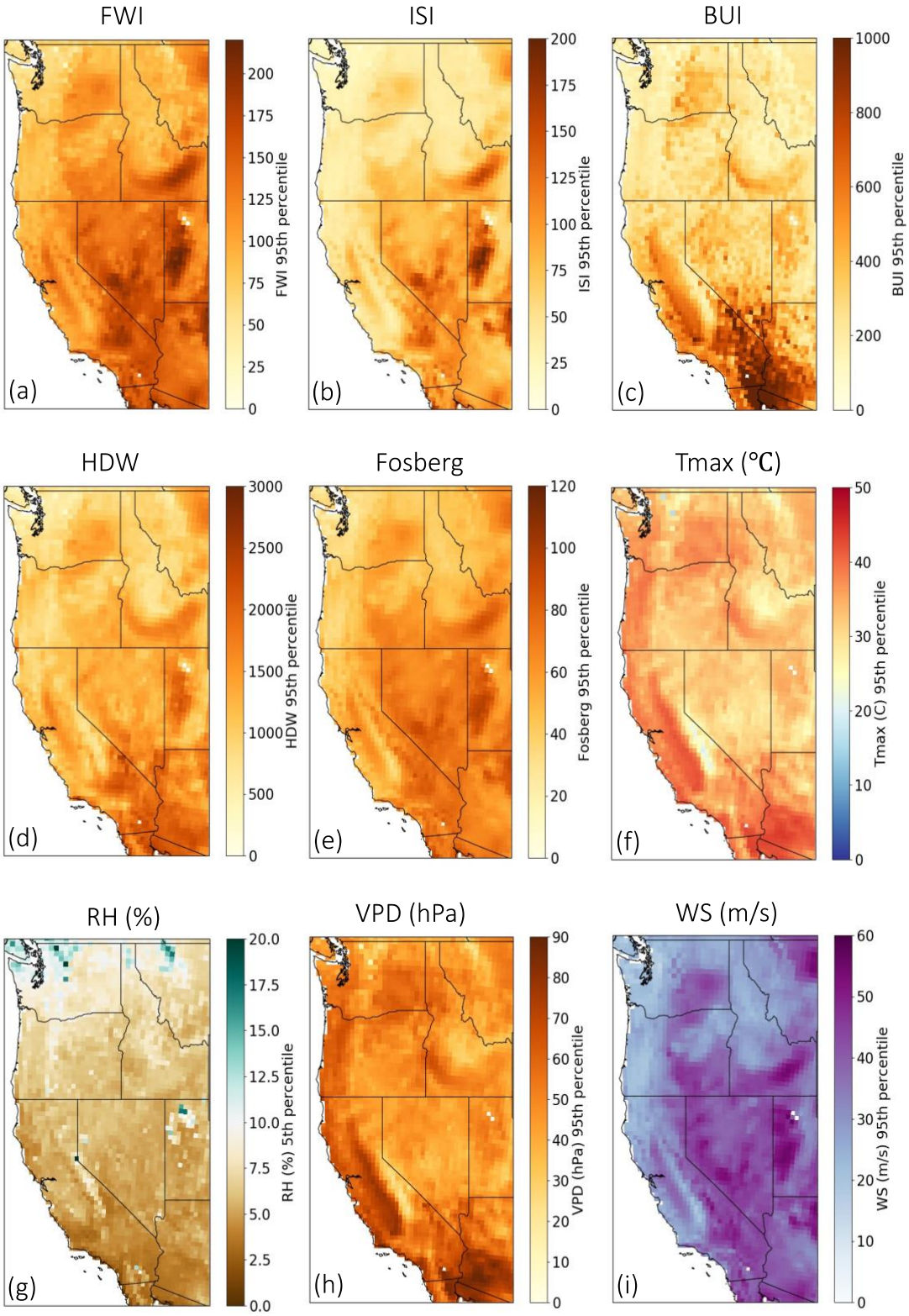

Figure S7. ActualClim ensemble 95th percentile of autumn (SON) maximum FWI and the concurrent fire weather indices and meteorological conditions by grid cell. For RH, the 5th percentile is shown.

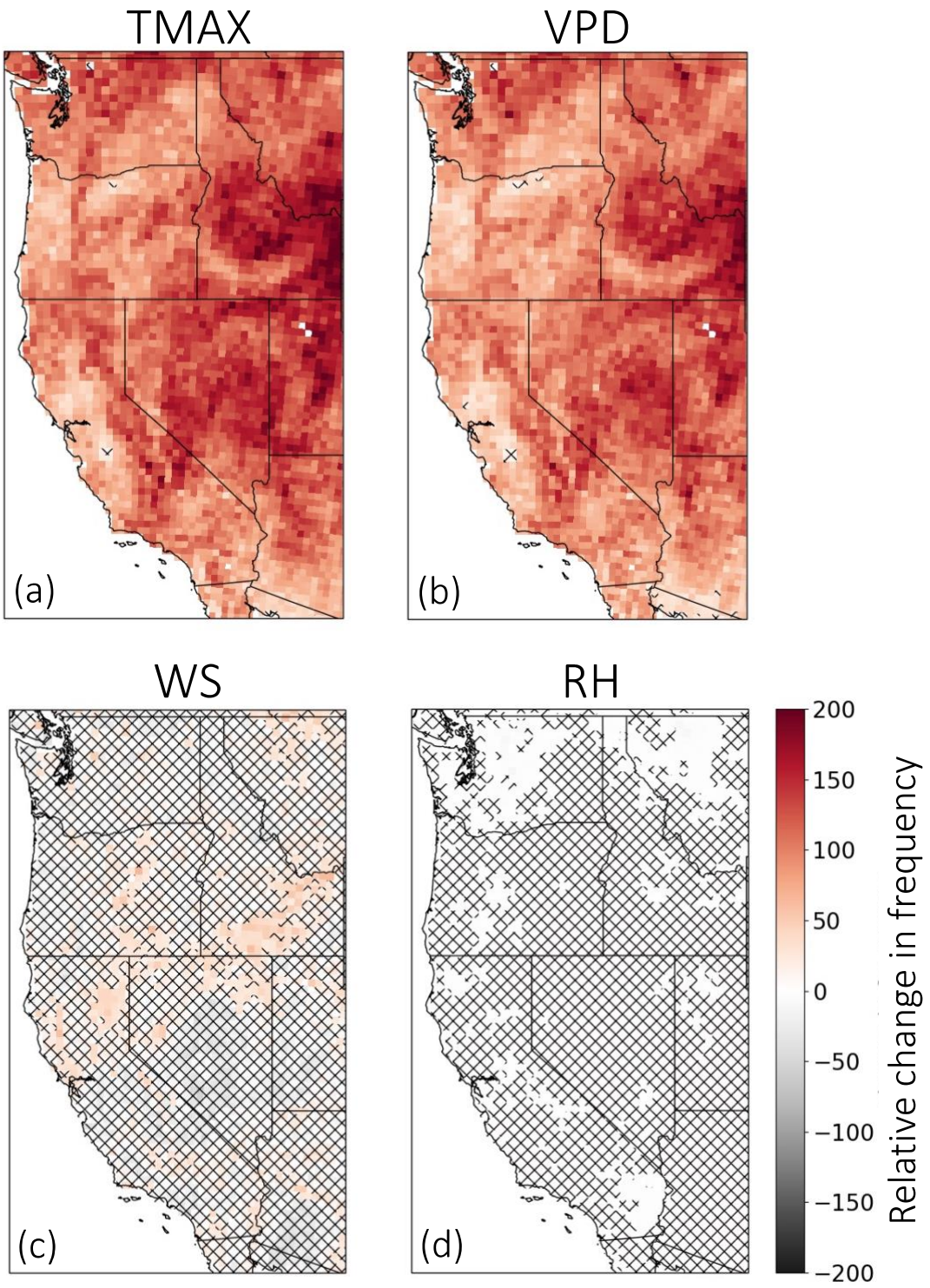

Figure S8. Relative change in frequency of extreme high (>95th percentile) autumn (SON) 21Z temperature (a) vapor pressure deficit (c) wind speed (d) and extreme low (<5th percentile) 21Z relative humidity (b) concurrent with the FWI_{max} between naturalClim and actualClim simulations.

Table S1. Summary of the simulated change in frequency (%) of fire weather indices and meteorological variables between actualClim and naturalClim ensembles, averaged over western US domain (approximately 35.2N–48.8N, 124W–109W).

Variable	Percent of domain with significant increases	Regional mean change in frequency
FWI	65%	+39%
ISI	52%	+27%
BUI	86%	+60%
HDW	99%	+105%
FFWI	20%	+9%
TA	99%	+117%
RH	18%	0%
VPD	99%	+105%
WS	11%	+4%

Table S2. Summary of the differences in meteorological variables in simulations where fire weather indices above the respective 95th percentile in actualClim and naturalClim ensembles, averaged over western US domain (approximately 35.2N–48.8N, 124W–109W).

Variable	Temperature (C)	Relative Humidity (%)	VPD (hPa)	Wind Speed (m/s)
FWI	1.15	0.10	1.52	-0.17
ISI	1.13	0.01	1.51	-0.08
BUI	0.97	0.11	1.21	0.25
HDW	1.11	-0.04	2.16	-0.07
FFWI	1.09	0.13	1.22	-0.04

Table S3. Difference (and fractional difference) in frequency between naturalClim and actualClim of Offshore Downslope Winds and Extreme Offshore Downslope Winds at 21 Z in the Autumn Fire Season (September-November).

Region	Variable	Natural forcings	All forcings	Anthropogenic effect	C.I.[c]
Offshore Downslope Winds					
ORa	Days per season	0.72	0.66	-0.06[a]	(-0.16,0.05)
	Probability	0.0080	0.0074	-0.08[b]	(-0.21,0.07)
ORb	Days per season	0.77	0.69	-0.08[a]	(-0.19,0.03)
	Probability	0.0086	0.0077	-0.10[b]	(-0.23,0.04)
CAa	Days per season	2.77	2.57	-0.19[a]	(-0.41,0.01)
	Probability	0.0308	0.0286	-0.07[b]	(-0.14,0.01)
CAb	Days per season	2.65	2.46	-0.19a	(-0.39,0.02)
	Probability	0.0294	0.0274	-0.07[b]	(-0.14,0.01)
CAc	Days per season	1.24	1.16	-0.09[a]	(-0.23,0.06)
	Probability	0.0138	0.0129	-0.07[b]	(-0.18,0.05)
CAd	Days per season	2.88	2.67	**-0.21[a]**	(-0.42,-0.01)
	Probability	0.0320	0.0297	**-0.07[b]**	(-0.14,-0.00)
Extreme Offshore Downslope Winds					
ORa	Days per season	0.09	0.09	0.00[a]	(-0.03,0.03)
	Probability	0.0010	0.0010	-0.01[b]	(-0.54,0.29)
ORb	Days per season	0.14	0.11	-0.03[a]	(-0.06,0.01)
	Probability	0.0015	0.0012	-0.19[b]	(-0.74,0.08)
CAa	Days per season	0.71	0.68	-0.03[a]	(-0.13,0.07)
	Probability	0.0079	0.0076	-0.04[b]	(-0.21,0.09)
CAb	Days per season	0.80	0.65	**-0.14[a]**	(-0.24,-0.04)
	Probability	0.0089	0.0073	**-0.18[b]**	(-0.40,-0.06)
CAc	Days per season	0.32	0.34	0.02[a]	(-0.05,0.09)
	Probability	0.0036	0.0038	0.06[b]	(-0.17,0.22)
CAd	Days per season	0.96	0.92	-0.04[a]	(-0.16,0.07)
	Probability	0.0107	0.0102	-0.05[b]	(-0.19,0.07)

[a]Difference: actualClim – naturalClim.

[b]Fractional difference: (actualClim – naturalClim) / naturalClim.

[a].[b]Bold-faced values have confidence intervals that do not include 0.

[c]95% confidence interval (C.I.)

Table S4. Difference (and fractional difference) between naturalClim and actualClim Near-Surface Conditions during Offshore Downslope Winds at 21 Z in the Autumn Fire Season (September-November).

Region	Variable	Natural Clim	Actual Clim	Anthropogenic effect	C.I.[c]
ORa	2-m temperature anomaly (°C)	-0.80	0.63	**1.43[a]**	(0.85,2.01)
	2-m relative humidity (%)	21.13	20.33	-0.04[b]	(-0.07,0.00)
	2-m vapor pressure deficit (kPa)	1.560	1.698	**0.09[b]**	(0.03,0.15)
	10-m wind speed (m s^{-1})	22.79	22.61	-0.01[b]	(-0.03,0.01)
ORa	2-m temperature anomaly (°C)	-0.09	0.90	**0.99[a]**	(0.42,1.54)
	2-m relative humidity (%)	18.26	17.86	-0.02[b]	(-0.06,0.02)
	2-m vapor pressure deficit (kPa)	1.903	2.016	**0.06[b]**	(0.00,0.12)
	10-m wind speed (m s^{-1})	16.29	16.40	0.01[b]	(-0.02,0.03)
CAa	2-m temperature anomaly (°C)	-1.57	-0.48	**1.09[a]**	(0.85,1.33)
	2-m relative humidity (%)	16.68	16.28	-0.02[b]	(-0.05,0.00)
	2-m vapor pressure deficit (kPa)	1.872	1.963	**0.05[b]**	(0.01,0.09)
	10-m wind speed (m s^{-1})	15.85	16.26	0.03[b]	(0.00,0.05)
CAb	2-m temperature anomaly (°C)	-1.24	-0.39	**0.85[a]**	(0.58,1.12)
	2-m relative humidity (%)	16.59	16.47	-0.01[b]	(-0.03,0.02)
	2-m vapor pressure deficit (kPa)	2.159	2.273	**0.05[b]**	(0.03,0.08)
	10-m wind speed (m s^{-1})	21.48	21.63	0.01[b]	(-0.01,0.03)
CAc	2-m temperature anomaly (°C)	-1.51	-0.68	**0.84[a]**	(0.49,1.18)
	2-m relative humidity (%)	17.48	17.19	-0.02[b]	(-0.05,0.02)
	2-m vapor pressure deficit (kPa)	1.872	1.963	**0.05[b]**	(0.01,0.09)
	10-m wind speed (m s^{-1})	16.92	16.94	0.00[b]	(-0.03,0.04)
CAd	2-m temperature anomaly (°C)	-1.44	-0.61	**0.83[a]**	(0.60,1.06)
	2-m relative humidity (%)	12.25	12.23	0.00[b]	(-0.03,0.03)
	2-m vapor pressure deficit (kPa)	2.374	2.486	**0.05[b]**	(0.02,0.07)
	10-m wind speed (m s^{-1})	29.56	29.73	0.01[b]	(0.00,0.02)

[a]Difference: all forcings – natural forcings.

[b]Fractional difference: (all forcings – natural forcings) / natural forcings.

[a,b]Bold-faced values have confidence intervals that do not include 0.

[c]95% confidence interval (C.I.)

Table S5. Difference (or fractional difference) between naturalClim and actualClim Near-Surface Conditions during Extreme Offshore Downslope Winds at 21 Z in the Autumn Fire Season (September-November).

Region	Variable	Natural Clim	Actual Clim	Anthropogenic effect	C.I.[c]
ORa	2-m temperature anomaly (°C)	-3.34	-0.98	**2.36[a]**	(0.60,4.03)
	2-m relative humidity (%)	15.67	13.89	**-0.11[b]**	(-0.18,-0.04)
	2-m vapor pressure deficit (kPa)	1.384	1.731	**0.25[b]**	(0.08,0.44)
	10-m wind speed (m s^{-1})	26.32	25.22	-0.04[b]	(-0.08,0.00)
ORa	2-m temperature anomaly (°C)	-1.98	-0.63	**1.35[a]**	(-0.18,2.82)
	2-m relative humidity (%)	14.0	13.31	-0.05[b]	(-0.13,0.03)
	2-m vapor pressure deficit (kPa)	1.653	1.878	0.14[b]	(-0.01,0.30)
	10-m wind speed (m s^{-1})	19.04	19.77	0.04[b]	(-0.01,0.09)
CAa	2-m temperature anomaly (°C)	-2.26	-0.87	**1.39[a]**	(0.98,1.79)
	2-m relative humidity (%)	12.96	13.01	0.00[b]	(-0.03,0.04)
	2-m vapor pressure deficit (kPa)	2.297	2.452	**0.07[b]**	(0.02,0.11)
	10-m wind speed (m s^{-1})	18.41	19.13	0.04[b]	(0.00,0.08)
CAb	2-m temperature anomaly (°C)	-1.77	-1.00	**0.77[a]**	(0.30,1.25)
	2-m relative humidity (%)	12.61	12.93	0.03[b]	(-0.01,0.06)
	2-m vapor pressure deficit (kPa)	2.194	2.223	0.01[b]	(-0.03,0.06)
	10-m wind speed (m s^{-1})	26.37	26.93	0.02[b]	(0.00,0.05)
CAc	2-m temperature anomaly (°C)	-1.51	-0.51	**0.99[a]**	(0.34,1.66)
	2-m relative humidity (%)	12.49	12.19	-0.02[b]	(-0.08,0.03)
	2-m vapor pressure deficit (kPa)	1.921	1.952	0.02[b]	(-0.04,0.08)
	10-m wind speed (m s^{-1})	22.19	22.33	0.01[b]	(-0.04,0.06)
CAd	2-m temperature anomaly (°C)	-2.87	-2.16	**0.71[a]**	(0.37,1.06)
	2-m relative humidity (%)	10.37	10.36	0.00[b]	(-0.04,0.04)
	2-m vapor pressure deficit (kPa)	2.144	2.213	0.03[b]	(0.00,0.07)
	10-m wind speed (m s^{-1})	32.75	33.15	0.01[b]	(0.00,0.03)

[a]Difference: all forcings – natural forcings.

[b]Fractional difference: (all forcings – natural forcings) / natural forcings.

[a],[b]Bold-faced values have confidence intervals that do not include 0.

[c]95% confidence interval (C.I.)